PERGAMON

Polyhedron 20 (2001) 1273–1277

POLYHEDRON

www.elsevier.nl/locate/poly

Preparation and magnetic properties of low symmetry $[Mn_4O_3]$ complexes with $S = 9/2$

Núria Aliaga [a], Kirsten Folting [a], David N. Hendrickson [b], George Christou [a,*]

[a] *Department of Chemistry and Molecular Structure Center, Indiana University, Bloomington, IN 47405-4001, USA*
[b] *Department of Chemistry, 0358 University of California at San Diego, La Jolla, CA 92093-0358, USA*

Received 17 September 2000; accepted 23 October 2000

Abstract

Controlled potential electrolysis (CPE) procedures have provided access to a family of distorted trigonal pyramidal $[Mn_4O_3(O_2CR)_4(dbm)_3]$ complexes (where R = C_6H_5 (**1**), C_6H_4-*p*-Me (**2**) and C_6H_4-*p*-MeO (**3**)) with an asymmetric $[Mn_4(\mu_3\text{-}O_3)(\eta^2,\mu_3\text{-}O_2CR)]^{6+}$ core. This results in C_s symmetry, lower than previous $[Mn_4O_3X(O_2CMe)_4(dbm)_3]$ complexes with C_{3v} symmetry. The dc magnetic susceptibility data of the C_s symmetry clusters are similar to those of the C_{3v} symmetry complexes, and fits of the data show a ferromagnetic coupling between Mn(III)–Mn(III) and antiferromagnetic coupling between the three Mn(III)–Mn(IV) pairs, giving a resultant $S = 9/2$ ground state. The out-of-phase ac susceptibility indicates slow magnetization relaxation and that these molecules are single-molecule magnets at low temperatures.

Keywords: Magnetic properties; Controlled potential electrolysis; $[Mn_4O_3]$ complexes

1. Introduction

Tetranuclear Mn compounds are important not only for their biological relevance but also for their ability to function as single-molecule magnets (SMM) at low temperatures [1]. Contrary to the majority of organic and inorganic compounds, many Mn clusters possess large number of unpaired electrons making them attractive as potential precursors to molecule-based magnetic materials or as discrete, nanoscale magnetic particles in their own right. During the last several years, our group has studied in detail the tetranuclear clusters $[Mn_4O_3X(O_2CMe)_3(dbm)_3]$ ($X = AcO^-$, Cl^-, Br^-, N_3^-, NCO^-, OH^-, MeO^- and dbm^- = the anion of dibenzoylmethane) of C_{3v} symmetry containing the $[Mn_4(\mu_3\text{-}O)_3(\mu_3\text{-}X)]^{6+}$ distorted-cubane core. It was discovered that these complexes possess a well isolated $S = 9/2$ ground state, exhibit slow relaxation of their magnetization, and display magnetization hysteresis, typical properties of single-molecule magnets [2]. The $[Mn_4O_3X]$ core of these systems is a trigonal pyramid of Mn ions with each face capped by O^{2-} or X^- ions. All of them have virtual C_{3v} symmetry in the solid state and in solution. In this paper, we describe related tetranuclear complexes with more bulky carboxylates (R = $^-O_2CC_6H_5$, $^-O_2CC_6H_4$-*p*-Me and $^-O_2CC_6H_4$-*p*-MeO), which have been synthesized by controlled potential electrolysis (CPE), as previously described for the R = Ph derivative [3]. These $Mn_4O_3(O_2CC_6H_4\text{-}p\text{-}R)_4(dbm)_3$ compounds have an unusual core structure, $[Mn_4(\mu_3\text{-}O_3)(\eta^2,\mu_3\text{-}O_2CR)]^{6+}$, that result in these molecules having a lower symmetry (C_s) in the solid state. In this paper are described the solid-state structural and the magnetochemical properties of these low symmetry manganese complexes.

2. Synthesis

2.1. Chemicals

All chemicals were used as received from Aldrich unless otherwise stated ($O_2CC_6H_5$ = benzoate; $O_2CC_6H_4$-*p*-Me = 4-methylbenzoate; $O_2CC_6H_4$-*p*-MeO = 4-methoxybenzoate; dbmH = dibenzylmethane). Sodium

* Corresponding author. Tel./fax: +1-812-855-2399.
E-mail address: christou@indiana.edu (G. Christou).

0277-5387/01/$ - see front matter
PII: S0277-5387(01)00605-2

dibenzylmethane, Nadbm·1/2H_2O and $NBu^n_4[Mn_4O_2(O_2CC_6H_5)_7(dbm)_2]$ (**4**), $NBu^n_4[Mn_4O_2(O_2CC_6H_4$-*p*-$Me)_7(dbm)_2]$ (**5**) and $NBu^n_4[Mn_4O_2(O_2CC_6H_4$-*p*-$MeO)_7(dbm)_2]$ (**6**) were prepared according to the literature methods [3–5].

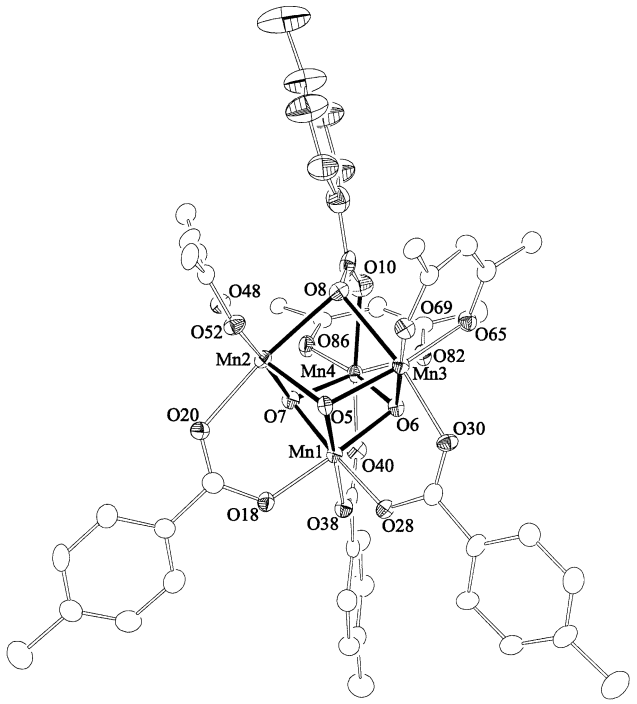

Fig. 1. ORTEP plot at the 50% probability level of $[Mn_4O_3(O_2CC_6H_4$-*p*-$Me)_4(dbm)_3]$ (**2**). For clarity, carbon atoms are represented as idealized spheres and only one phenyl carbon atom of each dbm^- group is shown.

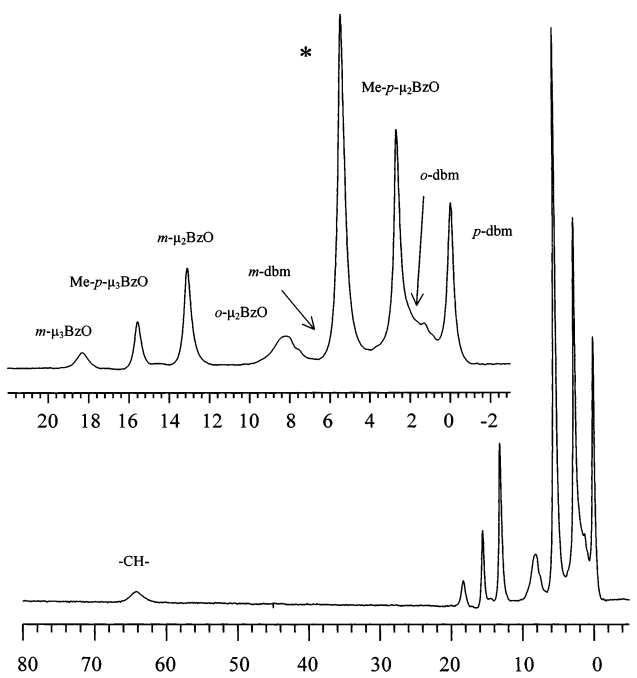

Fig. 2. ^1H NMR spectra in CD_2Cl_2 of $[Mn_4O_3(O_2CC_6H_4$-*p*-$Me)_4(dbm)_3]$. *, solvent impurity.

2.2. Electrochemistry

In controlled potential electrolysis, a fixed potential is applied while the current is monitored as a function of time. The accessible, quasi-reversible nature of the first oxidation process of $[Mn_4O_2(O_2CC_6H_4$-*p*-$R)_7(dbm)_2]^-$ has allowed the use of controlled potential electrolysis to oxidize one of the Mn(III) ions in **4**, **5** and **6** to Mn(IV). This oxidation is followed by a structural rearrangement to form complexes **1**, **2** and **3**. Complexes **4**, **5** and **6** were each dissolved in solutions of 0.1 M of $NBu^n_4PF_6$ in MeCN and electrolyzed. After ca. 1 h at an applied potential between 0.63 and 0.65 V versus Fc/Fc^+ a brown precipitate was observed in the solution. The poor solubility of the products simplifies their separation from each electrolysis reaction and the products were identified as **1**, **2** and **3**.

3. Results and discussion

The oxidation by CPE of $[Mn_4O_2]^{8+}$ (4Mn(III)) complexes to the trigonal pyramidal $[Mn_4O_3X]^{6+}$ (3Mn(III), Mn(IV)) clusters has been investigated with *para*-substituted benzoate groups. Complexes **1**, **2** and **3** have been identified by IR, ^1H NMR, elemental analysis, EPR and cyclic voltammetry; compound **2** was also characterized by X-ray crystallography. The core of these compounds is a tetra-face-capped Mn_4 trigonal pyramid containing hexacoordinated manganese atoms. This Mn_4 pyramid has a Mn(IV) ion at the apex, a μ_3-O^{2-} bridging each vertical Mn_3 face and a μ_3-benzoate group bridging the basal Mn_3 plane. This asymmetrically binding μ_3-benzoate ligand destroys the virtual C_{3v} symmetry of the entire molecule, leaving only a virtual mirror plane (virtual C_s symmetry). Each of the three Mn(III) ions displays a Jahn–Teller elongation axis, and these axes intersect at the μ_3-benzoate group. A plot of complex **2** is shown in Fig. 1; full details and metric parameters will be provided in the full paper [6].

3.1. ^1H NMR studies at room temperature

Complexes **1**, **2** and **3** possess virtual C_s symmetry in the solid state. However, ^1H NMR spectra in CD_2Cl_2 indicate higher solution symmetry (C_{3v}) for all three compounds. The ^1H NMR spectra show only one kind of dbm^- and two kinds of benzoate groups, the μ_3-benzoate ligand and three symmetry-related μ_2-benzoate ligands (Fig. 2). This suggests that there is a fluxional process occurring in solution that is fast on the ^1H NMR timescale, equilibrating the coordination mode of the oxygen atoms of the μ_3-benzoate ligand with the

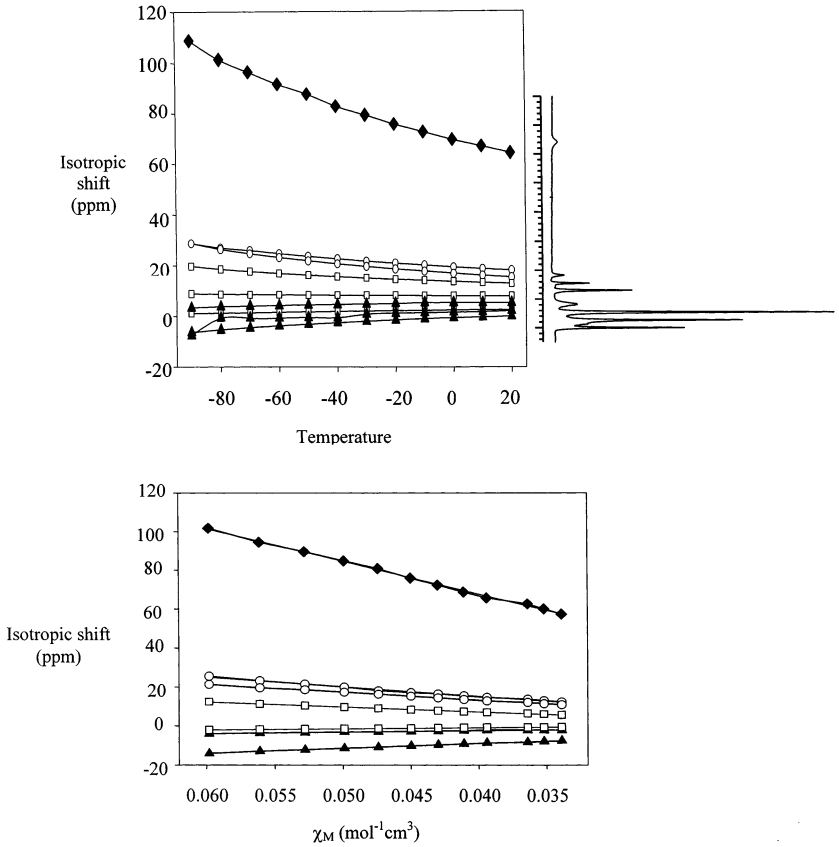

Fig. 3. Plots of the isotropic shifts of the dbm^- ligands vs. temperature (°C) (top) and the isotropic shifts of the dbm^- ligands vs. χ_M (bottom) for $[Mn_4O_3(O_2CC_6H_4\text{-}p\text{-}Me)_4(dbm)_3]$ (**2**).

three Mn(III) in the core of the complexes. Therefore, a C_3 axis is restored, and the effective solution symmetry increases.

The isotropic shift of a particular nucleus is the difference in resonance position between the paramagnetic complex and an equivalent diamagnetic complex. It is well-known that the isotropic shift has two components: the contact shift (when the interaction between the spin density and the resonating nucleus is through the bonding framework) and the dipolar shift (when this interaction is through space) [7]. In general, the π-delocalization mechanism can contribute to the contact shift when aromatic ligands are present in a paramagnetic complex. As a result, there is usually an upfield contribution to the isotropic shift at the *ortho* and *para* positions and a downfield contribution at the *meta* proton, and these do not necessarily attenuate with distance from the metal. The ^1H NMR spectra of these complexes were examined to verify an expected contact shift contribution to the isotropic shifts in the systems. Indeed, the spectra showed the alternating sign of the isotropic shift around the aromatic rings expected for a contact shift contribution via a π-delocalization mechanism.

Since the contact shift is proportional to the magnetic susceptibility, a linear relationship was expected in a variable-temperature study and this was observed (Fig. 3, bottom).

As the temperature was lowered, the ^1H NMR signals of compounds **1** and **2** in CD_2Cl_2 broadened but no decoalescence was observed. Thus, the fluxional process leading to effective C_{3v} symmetry cannot be slowed sufficiently to allow a lower symmetry to be manifest in the ^1H NMR spectrum.

3.2. Magnetochemistry

A variable-temperature magnetic susceptibility study was performed on polycrystalline samples of **1**, **2** and **3**. The magnetic susceptibility (χ_M) of these compounds was examined in a 10.0 kG field in the 2.0–300.0 K range (Fig. 4).

The effective magnetic moment of $[Mn_4O_3(O_2CC_6H_5)_4(dbm)_3]$ (**1**) increases from 8.08 μ_B at 300 K to a maximum of 9.63 μ_B at 30 K and then decreases to 6.48 μ_B at ca. 2 K. $[Mn_4O_3(O_2CC_6H_4\text{-}p\text{-}Me)_4(dbm)_3]$ (**2**) exhibits a similar behavior with the effective magnetic moment increasing from 8.53 μ_B at 300 K to a maximum of 9.76 μ_B at 30 K and then decreasing to 6.52 μ_B at ca. 2 K. In the case of $[Mn_4O_3(O_2CC_6H_4\text{-}p\text{-}MeO)_4(dbm)_3]$ (**3**) the effective magnetic

moment increases from 8.14 μ_B at 300 K to a maximum of 9.40 μ_B at 30 K and then decreases to 6.35 μ_B at ca. 2 K (Fig. 5). The decrease of the magnetic moment at low temperatures can be attributed to a combination of factors such as zero field splitting of the ground state and intercluster magnetic exchange interactions. At higher temperatures, the decrease is attributed to the thermal population of excited states.

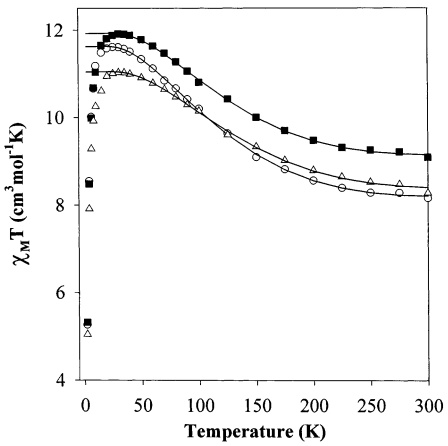

Fig. 4. Plot of the $\chi_M T$ (cm^3 mol^{-1} K) of complexes **1** (○), **2** (■) and **3** (△) vs. temperature (K). The solid lines represent the fit to the appropriate theoretical equation.

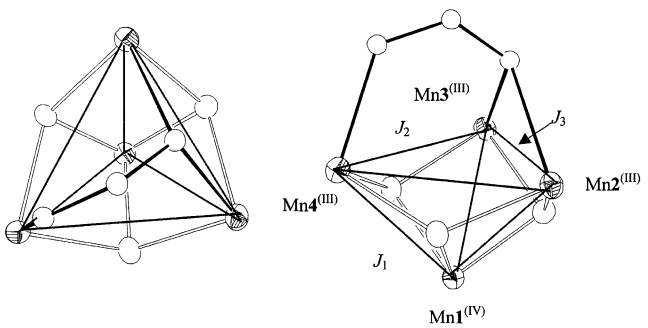

Fig. 5. Two diagrams of the core of complexes **1**, **2** and **3**, showing the labeling scheme for J_1, J_2 and J_3.

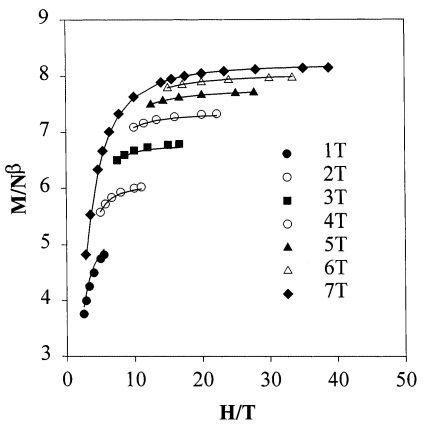

Fig. 6. Plot of $M/N\mu_B$ vs. H/T for $[Mn_4O_3(O_2CC_6H_4\text{-}p\text{-}Me)_4(dbm)_3]$ (**2**) at different fields of 1 T, 2 T, 3 T, 4 T, 5 T, 6 T and 7 T. The solid line represents the best fit as described in the text.

The data are similar to those for the related molecules with C_{3v} symmetry indicating the retention of an $S = 9/2$ ground state, as suggested by the μ_{eff} values at low temperature which are very close to the spin-only values expected for a $S = 9/2$ state. This is consistent with parallel alignment of the Mn(III) ($S = 2$) spins and antiparallel alignment of the Mn(IV) ($S = 3/2$) spin. The low symmetry of complexes **1**, **2** and **3** (C_s) needs to be considered in the fitting of the experimental magnetic susceptibility data to a theoretical χ_M versus T expression. The Kambe vector coupling method cannot be applied for these C_s symmetry systems without assuming all Mn(III) interactions are equivalent. Thus, approximation has been employed in order to simplify the equivalent operator approach and an excellent fit was subsequently obtained for all three of the compounds, as previously described for **1** [3]. Three J values need to be defined: J_1 describes the exchange interaction between Mn(III)–Mn(IV) pairs, and J_2 and J_3 describe the pairwise interactions between the three Mn(III) ions, of two types since only two of these ions are related by the virtual mirror plane of the molecule. The coupling scheme is shown in Fig. 5. The obtained values of the exchange parameters for **1**–**3** are in the ranges $J_1 = -23$ to -28 cm^{-1}, $J_2 = 3$–5 cm^{-1} and $J_3 = 0.5$–8 cm^{-1}. With the temperature independent paramagnetism (TIP) held constant at 800×10^{-6} cm^{-1}. In all three compounds, these parameters indicate a $S_T = 9/2$ ground state.

Variable-field magnetization data have been collected for **1**–**3** in the range of 1–7 T at low temperatures (1.8–25 K). In Fig. 6 is given a plot for complex **2** of the reduced magnetization, $M/N\mu_B$ (where N is Avogadro's number and μ_B is the Bohr magneton), versus the ratio of the magnetic field divided by the absolute temperature (H/T). The fitting of the experimental data was performed with a full matrix diagonalization routine. The results were $D = -0.65$ cm^{-1} and $g = 1.99$ for complex **1**, $D = -0.62$ cm^{-1} and $g = 1.92$ for complex **2**, and $D = 0.62$ cm^{-1} and $g = 1.85$ for complex **3**. An interesting observation is the D values of the $[Mn_4(\mu_3\text{-}O_3)(\eta^2,\mu_3\text{-}O_2CR)]^{6+}$ complexes: these values (0.62–0.65 cm^{-1}) are larger than all the $[Mn_4O_3X(O_2CMe)_3(dbm)_3]$ complexes with C_{3v} symmetry (ca. 0.30–0.45 cm^{-1}), and this fact can be directly related to the lower symmetry of compounds **1**–**3**.

Ac magnetic susceptibility data were collected for polycrystalline samples of **1**–**3** in the 1.8–10 K range with zero dc field and a 1.5 G ac field oscillating at either 99.7, 250, 497, 999 and 1488 Hz. For all three cases, the plots are very similar. As can be seen in Fig. 7(A) for complex **2**, at low temperatures there are clear signs of magnetic relaxation effects in the $\chi_M T$ versus temperature plot. For complex **2**, the plot of $\chi_M T$

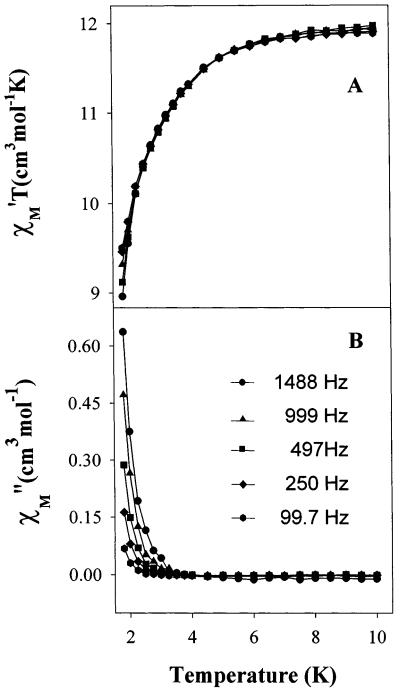

Fig. 7. Ac magnetic susceptibility data for complex **2** showing the in-phase (χ'_M) (A) and out-of-phase (χ''_M) (B) signals vs. temperature.

decreases from 11.70 $cm^3\ mol^{-1}$ K at ca. 5.5 K to 9.91 $cm^3\ mol^{-1}$ K at 1.8 K. For complex **1**, $\chi_M T$ decreases from 11.40 $cm^3\ mol^{-1}$ K at ca. 5.5 K to 8.96 $cm^3\ mol^{-1}$ K at 1.8 K and for complex **3**, $\chi_M T$ decreases from 10.40 $cm^3\ mol^{-1}$ K at ca. 5.4 K to 7.36 $cm^3\ mol^{-1}$ K at 1.8 K. In addition, an out-of-phase (χ''_M) ac signal appears and it is also frequency dependent (Fig. 7(B)). For all three compounds, χ''_M versus T plots do not show any peak maxima in the accessible T range (> 1.7 K). Lower temperature studies are in progress.

4. Conclusions

Control potential electrolysis allows the synthesis of a family of highly distorted trigonal pyramids $[Mn_4(\mu_3\text{-}O_3)(\eta^2,\mu_3\text{-}O_2CR)(\mu_2\text{-}O_2CR)_3(dbm)_3]$ complexes (where R = H, Me and MeO groups). These complexes have lower symmetry (C_s) than the $[Mn_4O_3X(O_2CMe)_3(dbm)_3]$ complexes studied previously (C_{3v}). However, magnetic studies show that complexes **1**, **2** and **3** maintain the same well isolated $S = 9/2$ ground state as previous $[Mn_4O_3X]^{6+}$ structures. The axial ZFS parameter, D, is found to be in the range -0.62 to -0.65 cm^{-1}, the largest values seen to date in $[Mn_4O_3X]^{6+}$ complexes.

5. Supplementary material

Crystallographic data for the structural analysis have been deposited with the Cambridge Crystallographic Data Centre, CCDC no. 154096. Copies of this information may be obtained from The Director, CCDC, 12 Union Road, Cambridge, CB2 1EZ, UK (fax: +44-1233-336033; e-mail: deposit@ccdc.cam.ac.uk or www: http://www.ccdc.cam.ac.uk).

Acknowledgements

This work was funded by the National Institutes of Health and the National Science Foundation.

References

[1] S.M.J. Aubin, N.R. Dilley, M.W. Wemple, M.B. Maple, G. Christou, D.N. Hendrickson, J. Am. Chem. Soc. 120 (1998) 839.
[2] S.M. Aubin, M.W. Wemple, D.M. Adams, J. Tsai, G. Christou, D.N. Hendrickson, J. Am. Chem. Soc. 118 (1996) 7746.
[3] S. Wang, M.S. Wemple, J. Yoo, K. Folting, J.C. Huffman, K.S. Hagen, D.N. Hendrickson, G. Christou, Inorg. Chem. 39 (2000) 1501.
[4] M.W. Wemple, H.-L. Tsai, S. Wang, J.P. Claude, W.E. Streib, J.C. Huffman, D.N. Hendrickson, G. Christou, Inorg. Chem. 35 (1996) 6437.
[5] S. Wang, J.C. Huffman, K. Streib, E.B. Lobkovsky, G. Christou, Angew. Chem. 103 (1991) 1681.
[6] N. Aliaga, K. Folting, D.N. Hendrickson, G. Christou, in preparation.
[7] S.D. Horrocks Jr, in: G.N. Lamar, W.D. Horrocks Jr (Eds.), Paramagnetic Molecules, Ch. 4, Academic Press, New York, 1973, pp. 159–161.